Supplemental Material

Michael Ortiz-Rios, Frederico A.C. Azevedo, Paweł Kuśmierek, Dávid Z. Balla, Matthias H. Munk, Georgios A. Keliris, Nikos K. Logothetis, Josef P. Rauschecker

Widespread and Opponent fMRI Signals Represent Sound Location in Macaque Auditory Cortex

Supplemental Figures

Overview

Figure/Table	Title
Figure S1	Auditory activation (sound vs. silence) of the auditory pathway in anesthetized and awake monkeys
Figure S2	Phase-mapping fMRI analyses and frequency maps of monkey M2
Figure S3	Spatial cues and phase peak response across cortical space
Figure S4	Positive and negative BOLD responses represent opponent hemifields
Figure S5	Cortical and subcortical hemifield tuning in awake monkey M4
Figure S6	RDM matrices of pairwise dissimilarity values (1 − Pearson *R*) between BOLD responses to each spatial sector
Figure S7	Matrix of RDM correlations (secondary RDM)
Figure S8	Spearman's coefficients between each cortical field RDM and hemifield code RDM

Table S1	Parameters of tuning to spatial positions for each CR of M1
Table S2	Parameters of tuning to spatial positions for each CR of M2

Figure S1. Auditory activation (sound vs. silence) of the auditory pathway in anesthetized and awake monkeys

(A) Activation maps (q FDR < 0.05, $p < 10^{-7}$, cluster size > 10 voxels) and time course examples of voxels in auditory cortex (AC), medial geniculate body (MGB) and inferior colliculus (IC) in anesthetized monkey M1. (B) Overall evoked activation in awake monkey M3 (q FDR < 0.05, $p < 7.8 * 10^{-5}$, cluster size > 10 voxels) and mean ± SEM time courses in AC. (C) Overall evoked activation in awake monkey M4 (q FDR < 0.05, $p < 5.6 * 10^{-3}$, cluster size > 10 voxels) and mean ± SEM time courses in AC.

Figure S2. Phase-mapping fMRI analyses and frequency maps of monkey M2

(A) Traveling wave design and stimulus presentation cycle (12 cycles/run). (B) The measure of coherence is equal to the amplitude of the BOLD signal modulation at the stimulus presentation rate (0.01 Hz for tonotopy, 0.0067 Hz for space mapping) divided by the square root of the power over all other frequencies except the harmonics. Voxels that exceeded a coherence value > 0.3 were then assigned a phase corresponding to the voxel's peak response to the stimuli presented in the cycle. (C) Coherence map used to threshold the phase map. (D) Resulting frequency maps and reversal boundaries (black dotted

lines) between the four identified regions. These included: Posterior (CL, CM), Primary (ML, A1, MM), Rostral (AL, R, RM) and Anterior (RTL, RT, RTM). ant, anterior; lat, lateral.

Figure S3. Spatial cues and phase peak response across cortical space

(A) Spectrogram of interaural level differences (L− R) of spatial stimuli within each sector obtained from left and right microphone signals. (B) Average interaural time delay between left and right stimuli for each sector and distance. (C) Phase peak value along cortical space spanning 10 mm across A1 orthogonal and parallel to the frequency axis shown for M1 (top) and M2 (bottom). (D) Tonotopy phase peak value (normalized to frequency range) along cortical space spanning 30 mm across AC parallel to the frequency axis shown for M1 for comparison to flat phase seen in C.

Figure S4. Positive and negative BOLD responses represent opponent hemifields

Activation t-maps with significant positive (red/yellow) and negative (blue) BOLD responses (q FDR < 0.05, $p < 10^{-4}$, cluster size > 10 voxels). Each map is shown next to the corresponding spatial sector in polar plots showing spatial tuning curves for each hemisphere of monkey M1. The spatial tuning curves were obtained from the spatial spread of the positive (red) and negative (blue) BOLD responses (PBRs and NBRs, respectively). Mean resultant vectors point towards the preferred angular direction, and the length represents the percentage of

active voxels around the mean direction. Negative angles (−180° - 0°) in the polar plot represent the left hemifield, while positive angles (+180° - 0°) represent the right hemifield.

Figure S5. Cortical and subcortical hemifield tuning in awake monkey M4

(A) Average cycles of voxels in auditory cortex (AC) and inferior colliculi (IC) of each hemisphere of monkey M4. Red dashed lines indicate duration periods of sounds presented in the right hemifield and blue dashed duration periods of sounds presented in the left hemifield. (B) Contrast t-maps (q FDR < 0.05, p < 10−2, cluster size > 10 voxels, t-value range ± 8.9) between all left and all right spatial sectors in awake monkey M4. Left image illustrates activations in AC and IC in the sagittal plane while right (up) and right (down) illustrates activation in the oblique axial plane of IC and AC, respectively. Voxels preferring the left hemifield sectors were mapped as negative (blue-to-cyan) while voxels preferring the right hemifield sectors were mapped as positive (red-to-yellow).

Figure S6. RDM matrices of pairwise dissimilarity values (1 − Pearson *R*) between BOLD responses to each spatial sector

This analysis was repeated for each cortical field of both left (A) and right (B) hemispheres (including AC). For the hemifield code RDM (C) we used the ITD delay functions for pair-wise correlations (**Figure S3B**) and linearly combined noisy estimates of the ITD RDMs with a categorical-model RDM (D). (E) Cortical RDMs compared to a hemifield model RDM above. The comparison was

conducted using stimulus-label randomization, and pair-wise comparisons among cortical RDMs (along with error bars) were based on bootstrap resampling of the stimulus set. Shaded gray bar illustrates the noise ceiling of the model, indicating the expected performance given the noise.

Figure S7. Matrix of RDM correlations (secondary RDM)

We calculated the distance (1 − Spearman correlation coefficient) between RDMs shown in **Figure S6**. Note that the RDM from the right posterior region correlates best with the hemifield code RDM.

Figure S8. **Spearman's coefficients between each cortical field RDM and hemifield code RDM**. (A-D) Bar histogram of individual Spearman's correlation coefficients between Hemifield code RDM and CF's RDMs from each hemisphere for each individual run of monkeys M1-M4, respectively. Red color bars indicate highest correlation coefficients between CF and hemifield code RDMs. For the awake monkey's boundaries and regions were obtained from anatomical reference (Saleem and Logothetis, 2012). (E) Mean ± SEM of correlation coefficients for each monkey.

Table S1. Parameters of tuning to spatial positions for each CR in monkey M1

CF	*N voxels*	*mean tuning direction*	*SD (circular)*	*Upper CI*	*Lower CI*
Lh Posterior	1452	124	63.0	132.3	116.3
Lh Primary	744	110	72.2	123.9	96.8
Lh Rostral	434	118	55.6	124.3	112.3
Lh Anterior	521	124	55	130.1	118.6
Rh Posterior	1549	-94	53.8	-87.6	-101.4
Rh Primary	709	-143	69.3	-132.3	-153
Rh Rostral	486	-120	57.3	-114	-126
Rh Anterior	454	-111	61.3	-103.7	-119.2

Table S2. Parameters of tuning to spatial positions for each CR in monkey M2

CF	*N vox*	*mean tuning direction*	*SD (circular)*	*Upper CI*	*Lower CI*
Lh Posterior	1036	108	66.5	117.4	98.5
Lh Primary	582	108	69.3	117.4	98
Lh Rostral	319	97	57.3	104.3	90.5
Lh Anterior	212	99	55.6	106	-91.7
Rh Posterior	946	-82	49.8	-76.2	-87
Rh Primary	604	-118	69.9	-106.6	-128.3
Rh Rostral	430	-101	63	-92.8	-108.8
Rh Anterior	224	-101	56.1	-94.5	-107.1

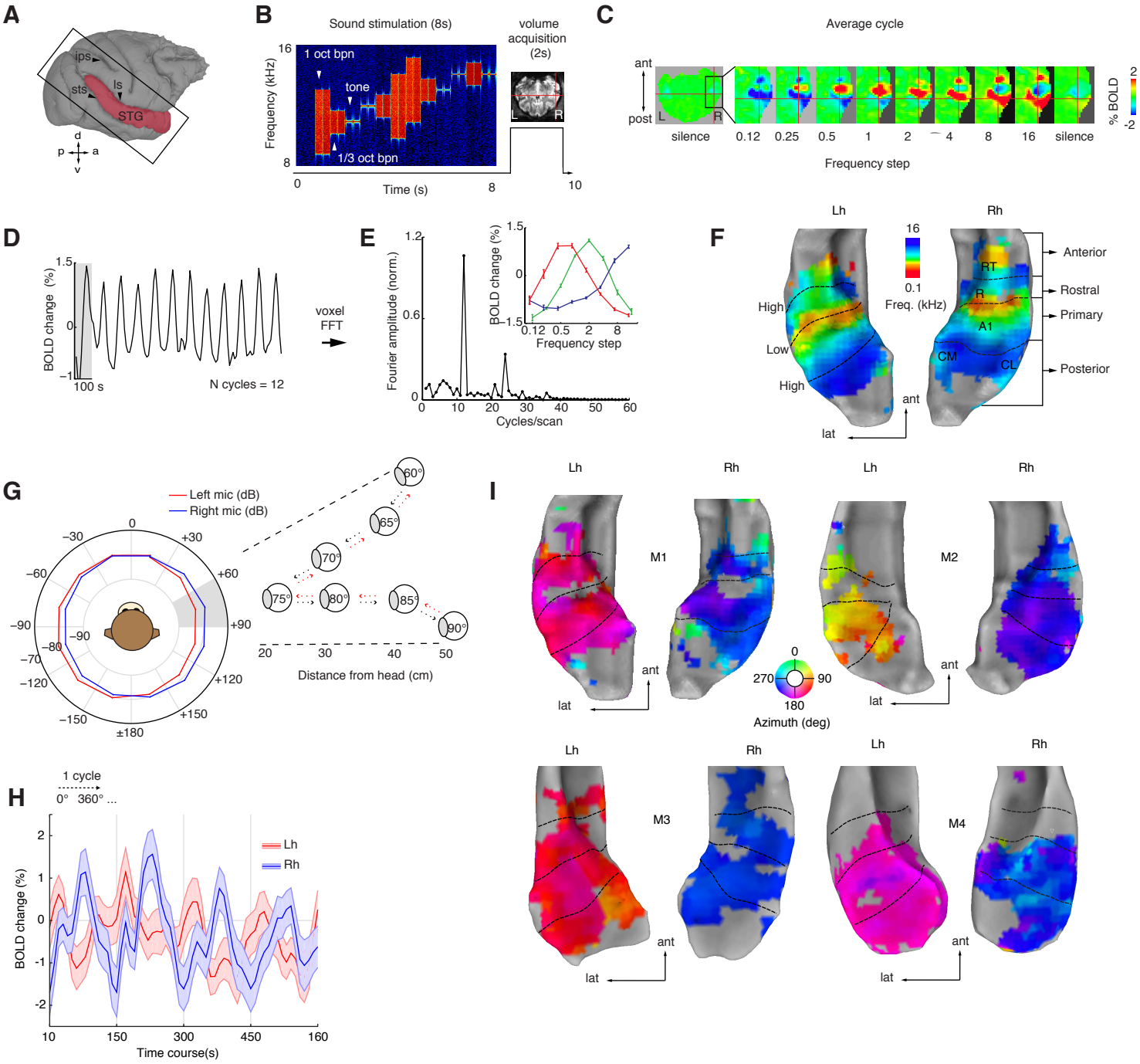

Figure 1. Phase-mapping for frequency and space

(A) Image acquisition plane and extracted surface (red). (B) Sparse imaging and stimulation design (e.g. high frequency stimuli, 8-16 kHz). (C) Average BOLD response to each frequency step in octaves (labeled frequency refers to the upper range of the frequency presented). (D) Time course of a voxel in A1 (crosshair in C) tuned to high frequency. Gray shading represents one presentation cycle. (E) Fourier transform of the same voxel's shows a peak at the stimulation rate (0.01 Hz = 12 cycles/1200 s). Inset panel, mean ± SEM of 3 voxels in A1 at the peak stimulation rate. Response peaks were used to calculate the preferred phase that translates to preferred sound frequency independently at each voxel. (F) Resulting tonotopic maps rendered into STG surfaces of each hemisphere. Black dotted lines indicate frequency-reversal boundaries of preferred sound frequency between mirror-symmetric regions. For the awake monkeys (M3 and M4) reversal boundaries were obtain anatomical reference (Saleem and Logotheis, 2008) (G) Binaural sound recordings and stimulation design. Mean amplitude of sounds (broad-band noise 0.125-16 kHz) recorded at each ear (red and blue) plotted in hemifield polar angles. Outset panel illustrates a virtual sector of speaker orientations and distances from the head. Sounds bursts (100 ms) were played every 5° in a leftward, rightward and distance sequence oscillating pattern (dashed red and black arrows) within a 30°-wide spatial sector (shaded gray, n sectors = 12) for 7.2s. (H) Mean and ± SEM of BOLD signal in all significant voxels (coherence > 0.3) in AC shown for four cycles of the time course to illustrate the overall broad amplitude modulation across hemispheres. (I) Space maps at the stimulation rate (0.0067 Hz = 12 cycles/1800 s) highlights two phases across hemispheres in all four monkeys. STG, superior temporal gyrus; ls, lateral sulcus; ips, intraparietal sulcus; sts, superior temporal sulcus; Lh, left hemisphere; Rh, right hemisphere; ant, anterior; lat, lateral; post, posterior.

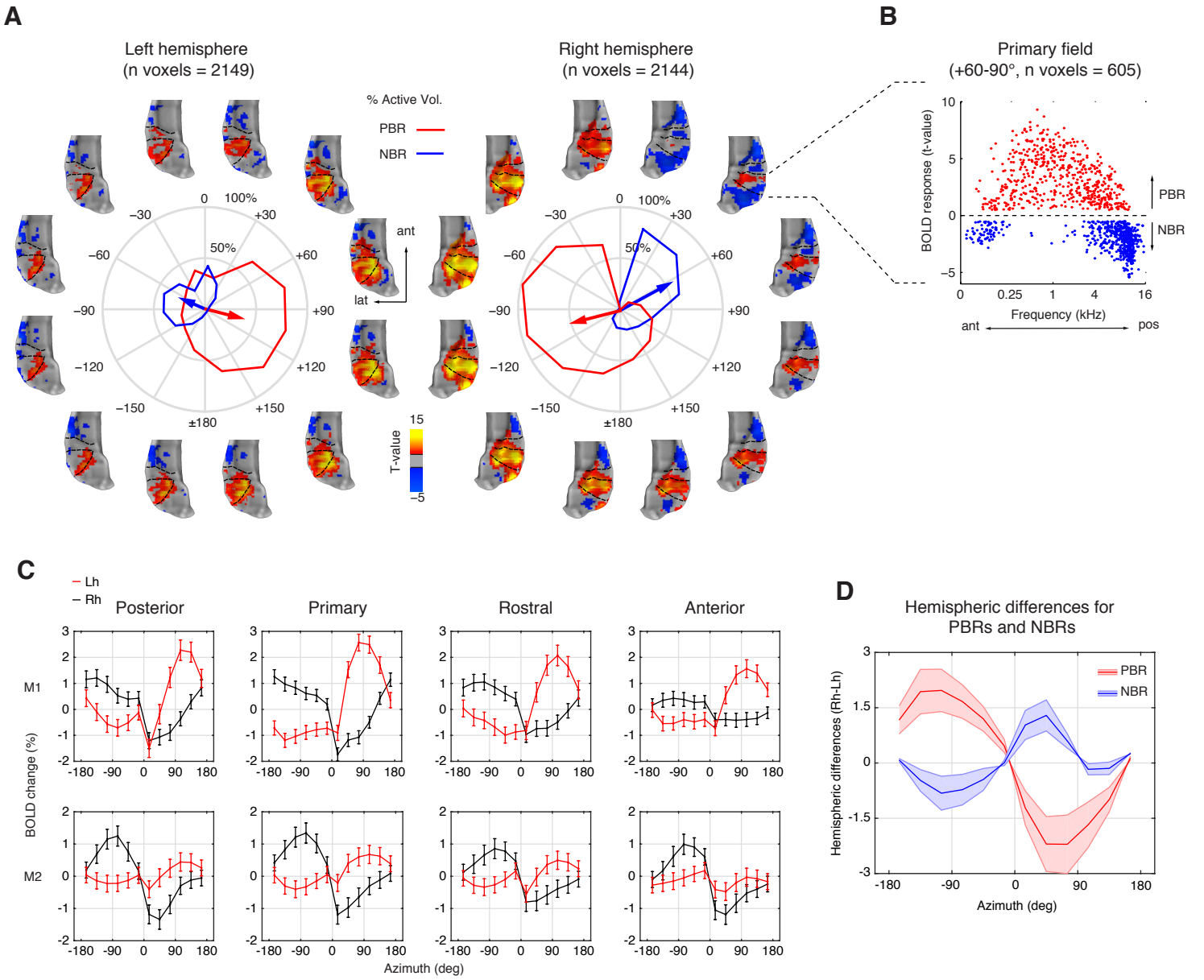

Figure 2. Positive and negative BOLD responses represent opposite hemifields
(A) Activation t-maps with significant positive (red/yellow) and negative (blue) BOLD responses (q FDR < 0.05, p < 10−6, cluster size > 10 voxels). Each map is shown around the corresponding spatial sector in polar plots of each hemisphere of monkey M2 (see **Figure S4** for a similar plot in monkey M1). The polar plot shows spatial tuning curves obtained from the spatial spread of the positive (red) and negative (blue) BOLD responses (PBRs and NBRs respectively). Mean resultant vectors (arrows) point towards the preferred angular direction. The length represents the percentage of active voxels around the mean direction. Negative angles (−180° - 0°) in polar plot represent the left hemifield and positive angles (+180° - 0°) the right hemifield. (B) Scatterplot of voxels in primary field showing PBRs and NBRs to an exemplar spatial sector (+60° - 90°) plotted as function of the frequency tuning of each voxel. (C) Mean and ± SEM of BOLD responses (including both PBRs and NBRs) for cortical regions of each hemisphere (Lh, red; Rh, black) of monkey M1 (top) and M2 (bottom). (D) Average amplitude differences across hemispheres for PBRs and NBRs plotted as a function of azimuth. The differential response shows opposite polarity between hemifields with a peak in NBRs for frontal right sectors. Lh, left hemisphere; Rh, right hemisphere; ant, anterior; pos, posterior.

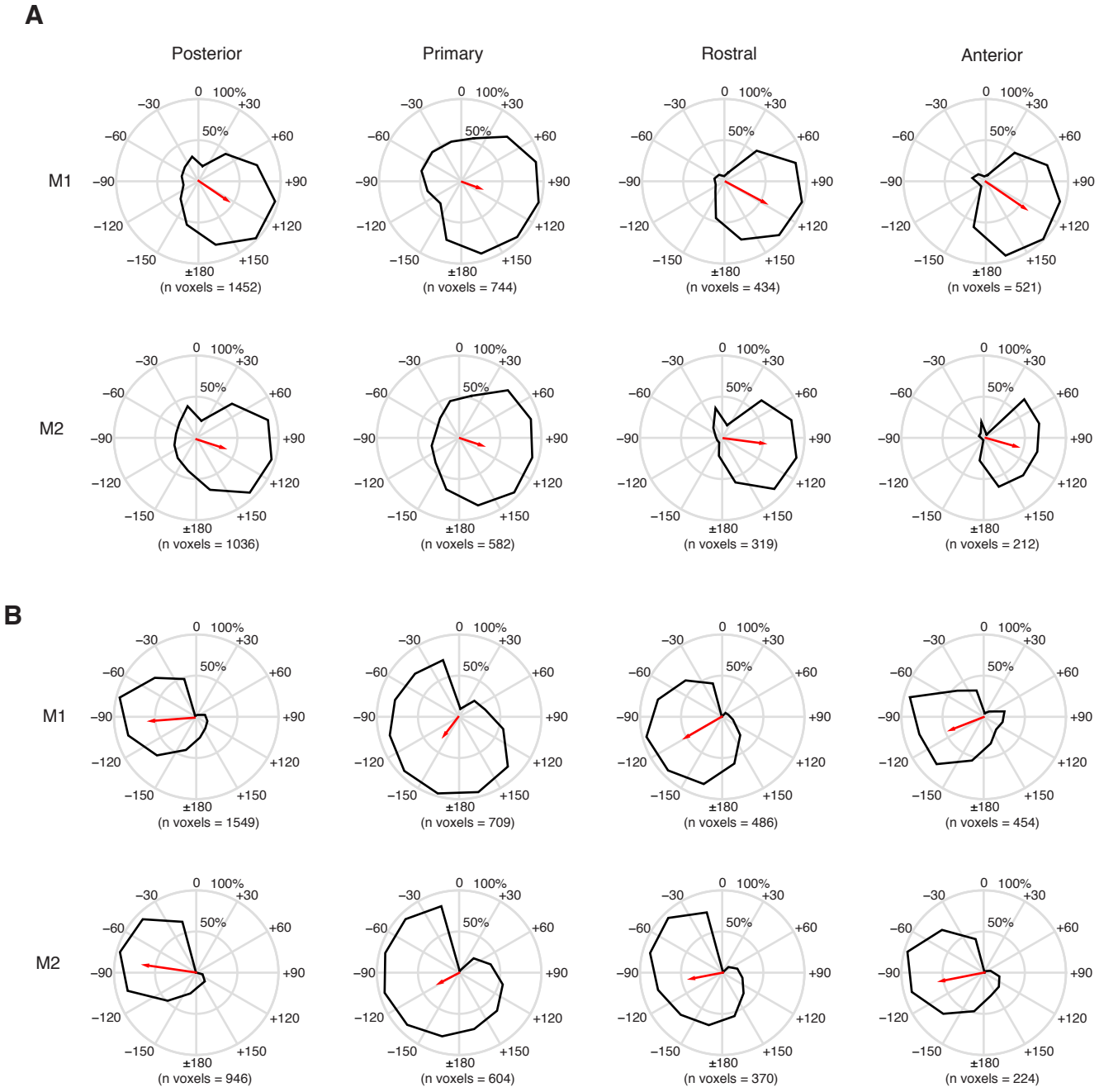

Figure 3. Cortical fields are broadly tuned to contralateral space

The spatial spread of the positive BOLD response was used to calculate spatial tuning curves (black curves) for each cortical field: Posterior, primary, rostral and anterior. (A) Left hemisphere for M1 (top panel) and M2 (bottom panel). (B) Right hemisphere for M1 (top panel) and M2 (bottom panel). The mean resultant vectors (red) point towards the preferred circular mean direction, and the length represents the percentage of active voxels concentrated around ± 30° of the mean direction. All fields were approximately oriented around ± 90° - 120°. Overall, cortical fields were broadly tuned, with central fields (primary and rostral) slightly broader than anterior and posterior fields (see **Table S1, S2**).

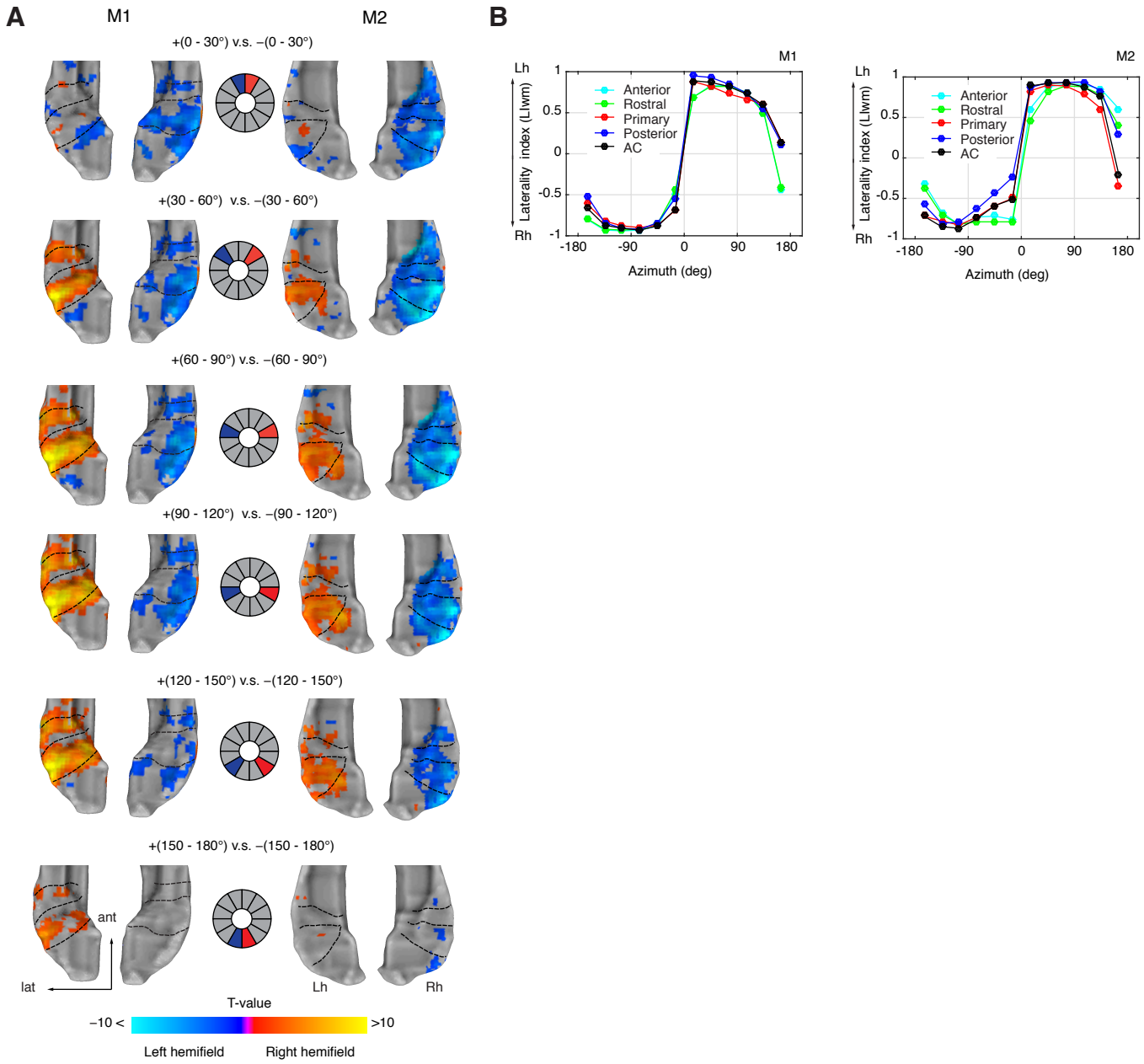

Figure 4. Auditory cortex represents the contralateral hemifield

(A) Contrast t-maps between equidistant sectors for both monkeys. Middle panel illustrates the contrast design between sectors (left hemifield in blue; right hemifield in red). Voxels preferring left hemifield sectors were mapped as negative (blue-to-cyan) while voxels preferring right hemifield sectors were mapped as positive (red-to-yellow). The range of t-values (q FDR < 0.05, p < 10−3, cluster size > 10 voxels) in the color bar was scaled according to a maximum t-value of 10 to illustrate the strength of the contrast across sectors and monkeys. (B) Mean-weighted laterality index (LIwm) between hemispheres calculated from the t-value threshold of each spatial sector (see **Experimental Procedures**). Index range between −1 and +1 with a positive value indicating Lh biases and a negative index indicating Rh biases. Index curves are shown for each monkey and for each cortical field, including auditory cortex as a whole (all fields combined). Lh, left hemisphere; Rh, right hemisphere.

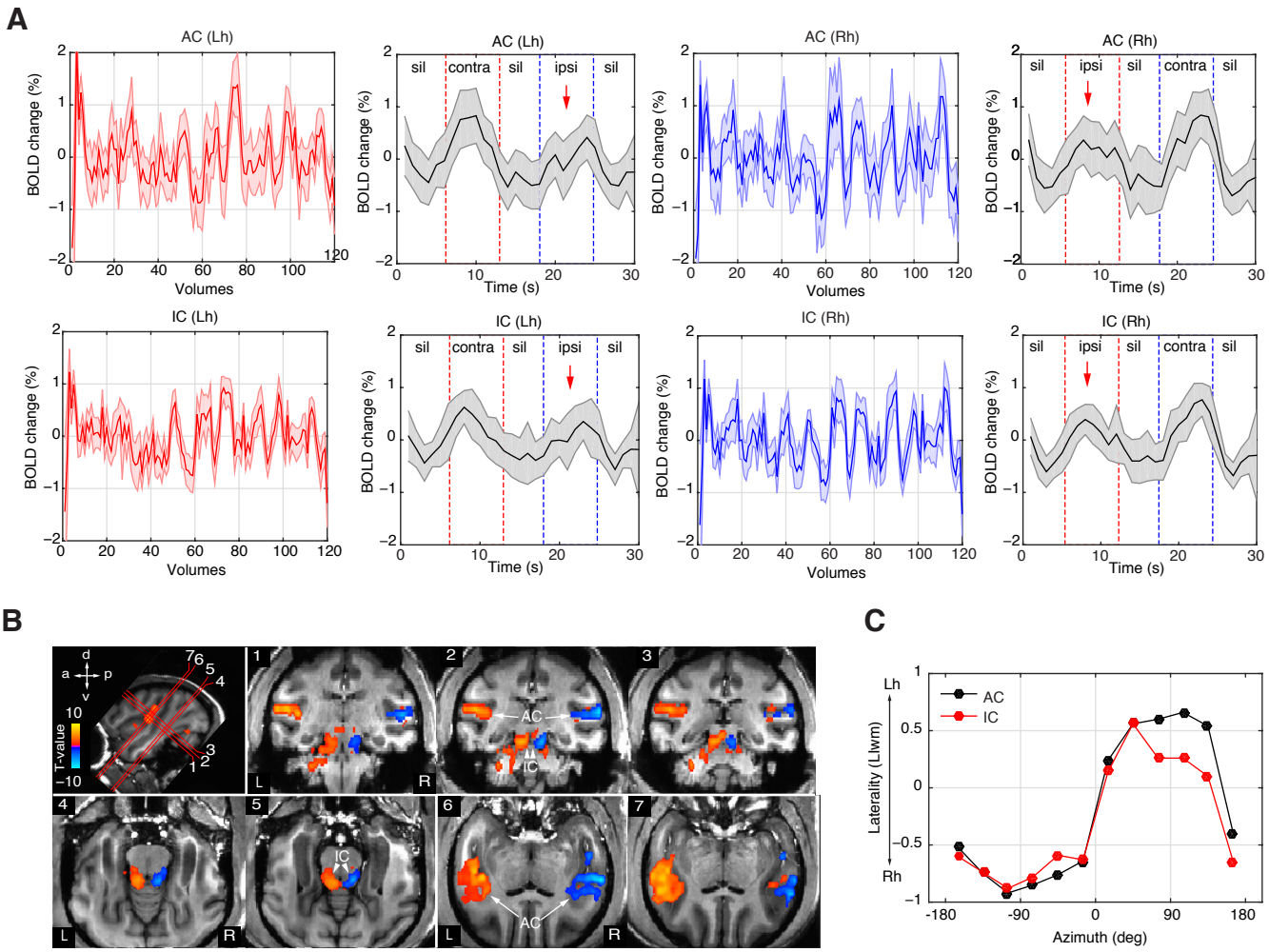

Figure 5. Cortical and subcortical hemifield tuning in the awake monkey
(A) Example time courses and average cycles of voxels in auditory cortex (AC) and inferior colliculi (IC) of each hemisphere. Red dashed lines indicate duration periods of sounds presented in the right hemifield and blue dashed duration periods of sounds presented in the left hemifield. Notice the amplitude suppression for sounds sources in the ipsilateral side (red arrows). (B) Contrast t-maps (q FDR < 0.05, p < 10−3, cluster size > 10 voxels, t-value range ± 7.8) between all left and all right spatial sectors in awake monkey M3. Top left image illustrates oblique slice orientations and planes (numbered 1-7) cutting through AC and IC. Voxels preferring the left hemifield sectors were mapped as negative (blue-to-cyan) while voxels preferring the right hemifield sectors were mapped as positive (red-to-yellow). (C) Laterality index (LIwm) curves for AC and IC of monkey M3. Contra, contralateral; ipsi, ipsilateral; sil, silence.

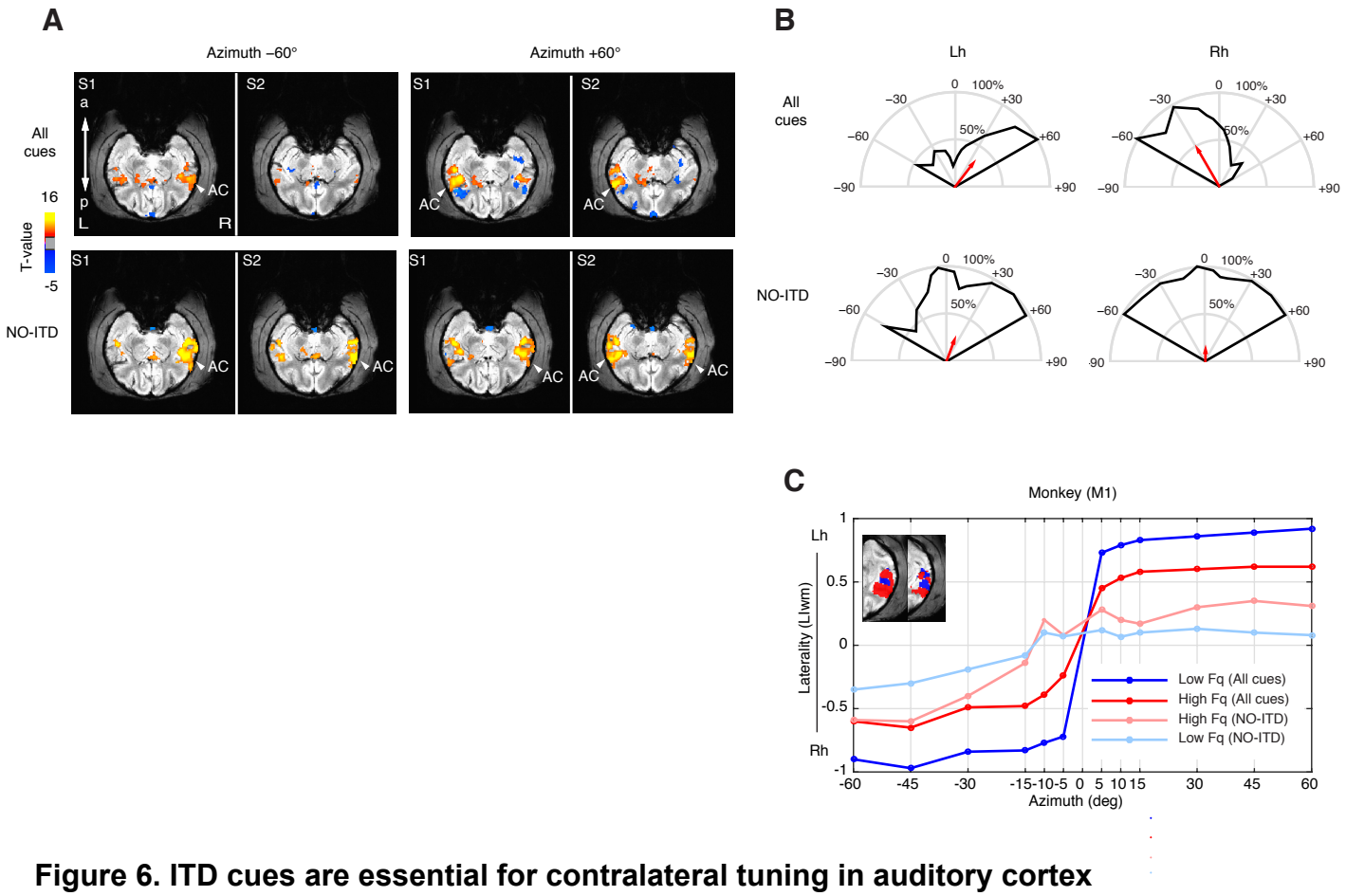

Figure 6. ITD cues are essential for contralateral tuning in auditory cortex
(A) Example t-maps with significant BOLD responses (q FDR < 0.05) to spatial sounds presented in left (+60°) and right (−60°) hemifields. “All cues” condition (top panel) and “NO-ITD” condition (bottom panel) in which ITD cues were removed from the original recorded sounds, leaving ILD and spectral cues. Maps are shown for two pairs of oblique slices (S1 ventral and S2 dorsal) cutting through the superior temporal gyrus. The response to rightward +60° in the NO-ITD condition was observed in both auditory cortices (i.e., no contralateral tuning). (B) Spatial tuning curves for frontal field show a loss of hemifield tuning in the right hemisphere for the NO-ITD condition. (C) Laterality index (LIwm) as a function of frontal azimuth plotted for low and high frequency voxels shows a lack of laterality (LIwm near zero) for sounds without ITD at the midline (± 15°) with only a slight increase in laterality for high frequency (LIwm < 0.5) as compare to low frequency in more lateral sectors.

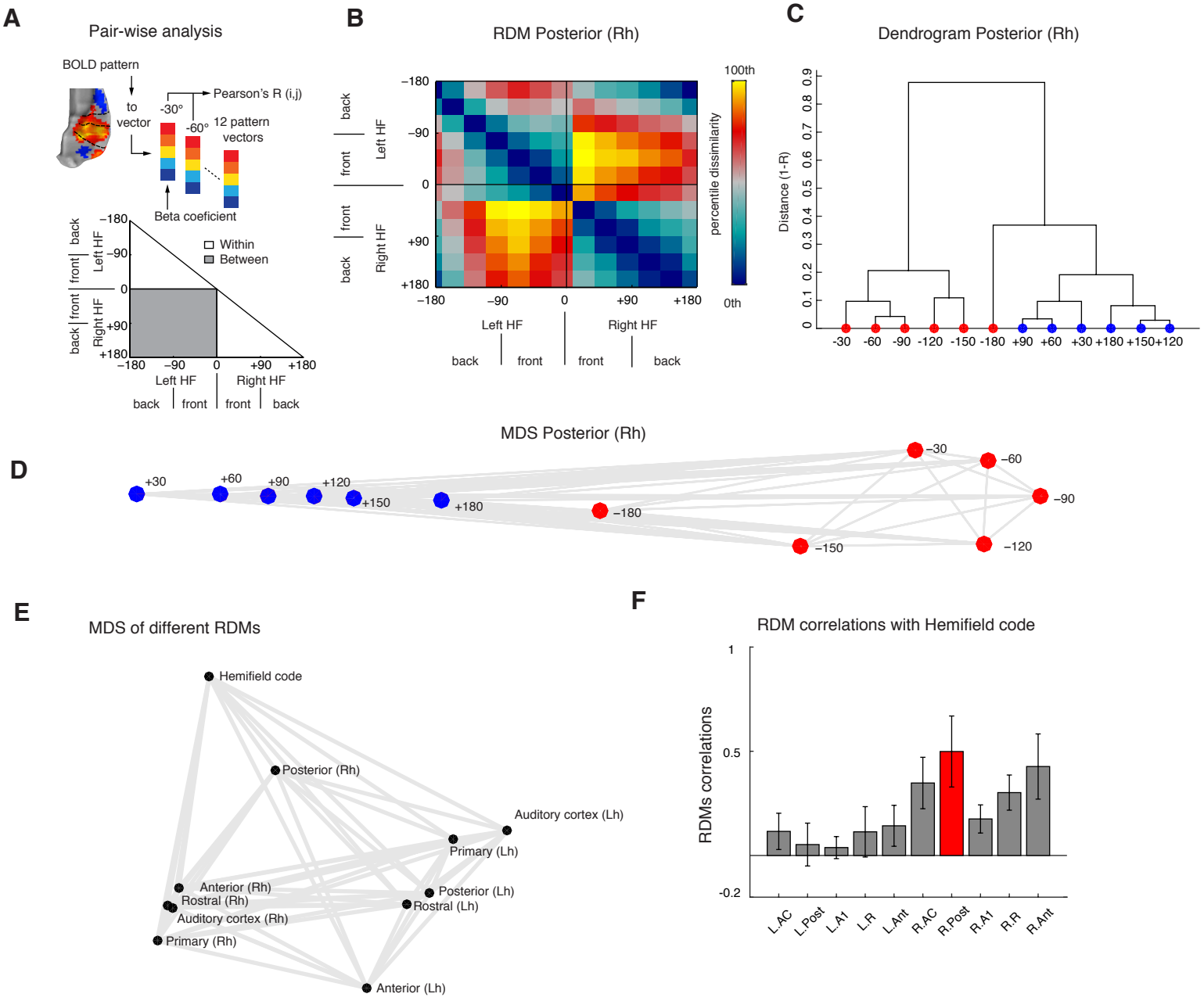

Figure 7. Posterior superior temporal region (pST) represents space similarly to a hemifield code
(A) For each field we extracted the response patterns to each spatial sector, yielding 12 response patterns. We then calculated pairwise Pearson's correlations (R) across all spatial sectors and then assigned the dissimilarity measure (1 − R) to a 12 x 12 representational dissimilarity matrix (RDM). This analysis was repeated for each cortical field and the hemifield model for all runs and monkeys (see Figure S5). (B) Mean RDM of the right pST region. The color bar reflects dissimilarity in percentiles (low dissimilarity, blue; high dissimilarity, red/yellow). (C) Hierarchical clustering and (D) multidimensional scaling (MDS) of fMRI responses in right pST. Unsupervised hierarchical clustering (criterion: average dissimilarity) revealed a hierarchical structure dividing left and right hemifields. MDS (criterion: metric stress) resulted in apparent segregation of data derived from each hemifield (red vs. blue). (E) MDS based on dissimilarity (1 − Spearman's correlation) between RDMs (see Figure S6 for second-order RDM). Visual inspection of the MDS structure reveals that the right pST RDM lies closer to the hemifield model than any other cortical region. (F) Mean and ± SEM of Spearman's correlation coefficients obtain from all monkeys and runs (n = 65) between CFs and hemifield code (see Figure S7 for individual runs and monkeys) RDMs. RDM from the right pST relates more to the hemifield code than any other RDM.

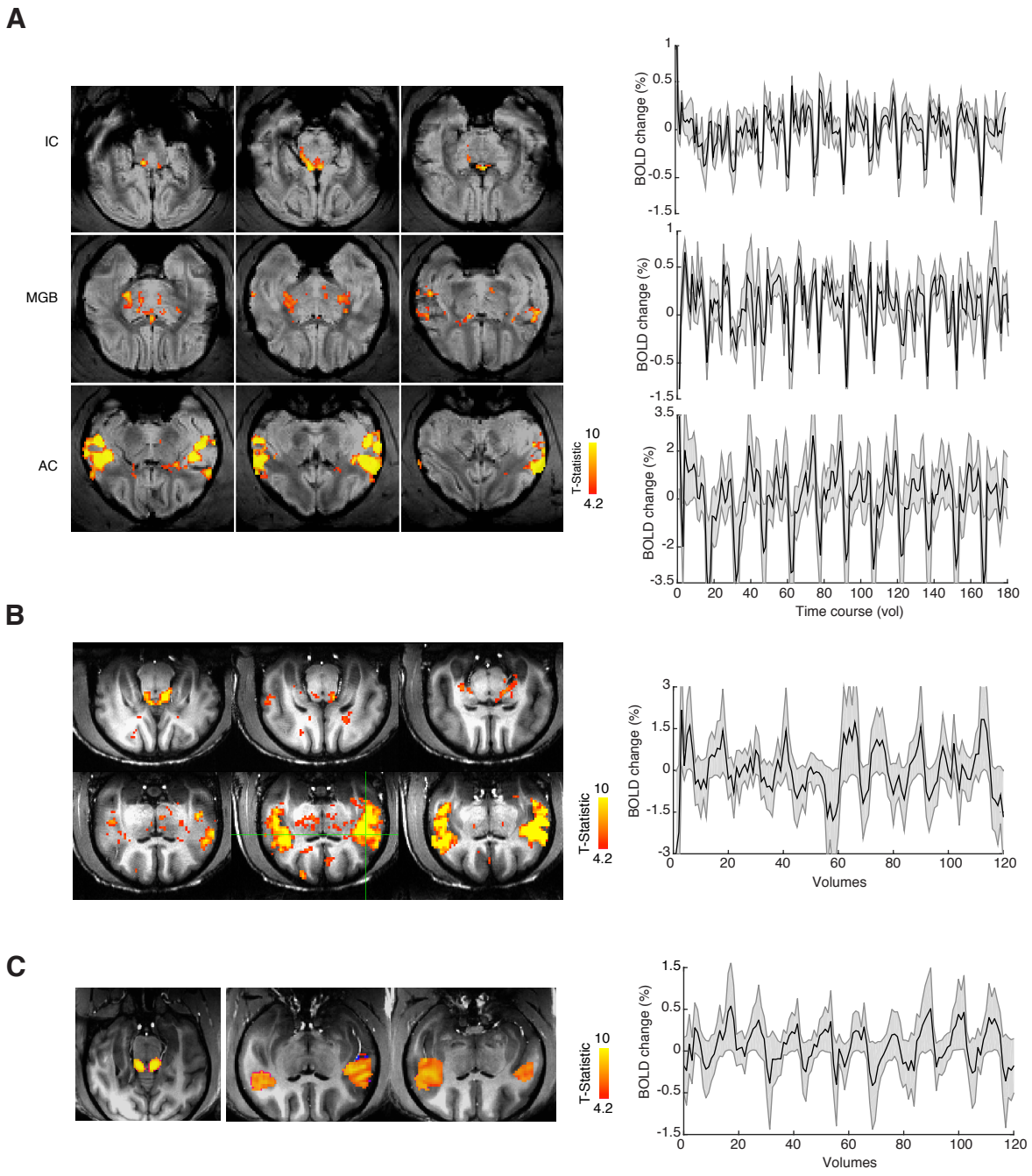

Figure S1. Auditory activation (sound vs. silence) of the auditory pathway in anesthetized and awake monkeys

(A) Activation maps (q FDR < 0.05, p < 10−7, cluster size > 10 voxels) and time course examples of voxels in auditory cortex (AC), medial geniculate body (MGB) and inferior colliculus (IC) in anesthetized monkey M1. (B) Overall evoked activation in awake monkey M3 (q FDR < 0.05, p < 7.8 * 10−5, cluster size > 10 voxels) and mean and ± SEM time courses in AC.(C) Overall evoked activation in awake monkey M4 (q FDR < 0.05, p < 5.6 * 10−3, cluster size > 10 voxels) and mean and ± SEM time courses in AC.

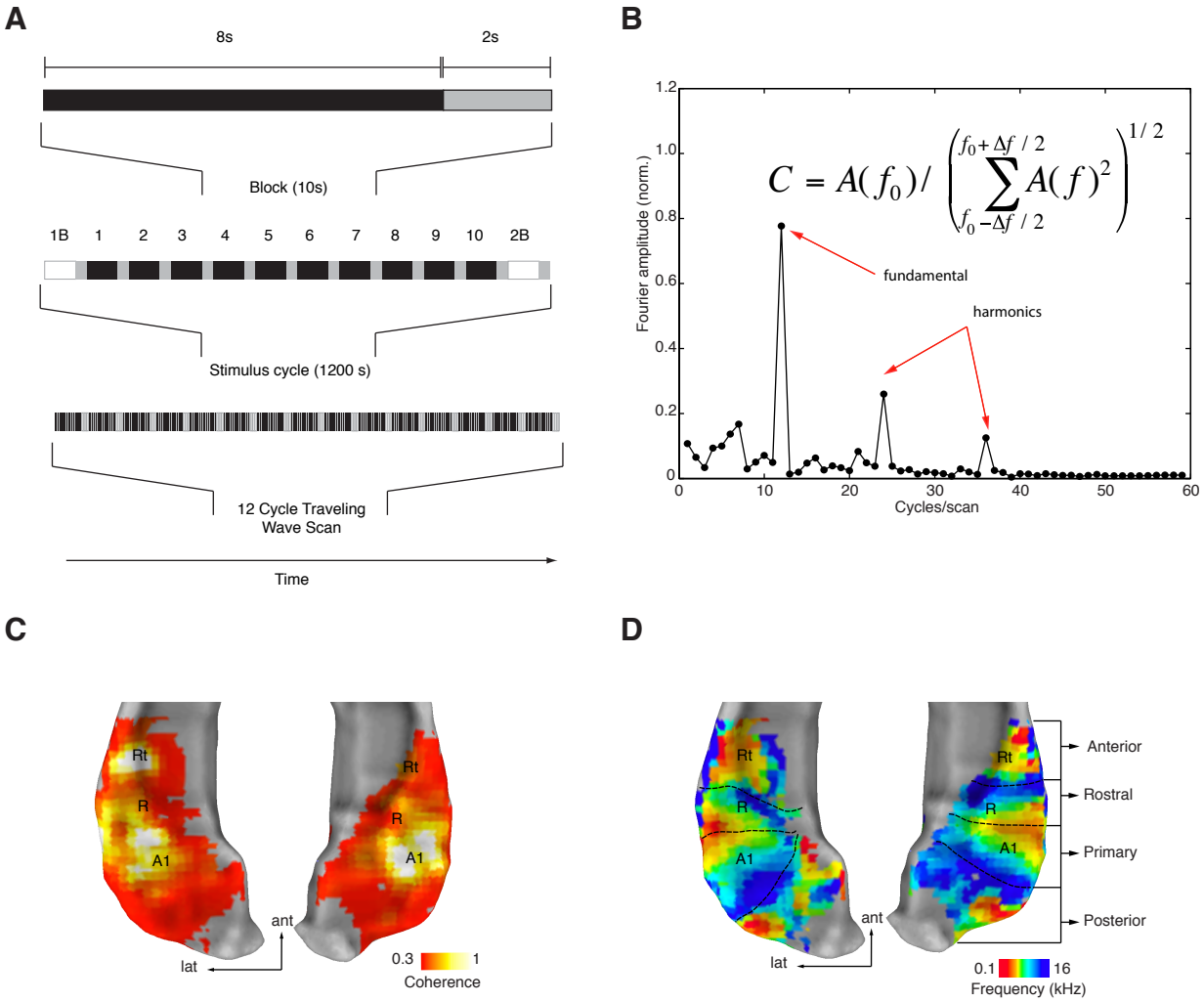

Figure S2. Phase-mapping fMRI analyses and frequency maps of monkey M2
(A) Traveling wave design and stimulus presentation cycle (12 cycles/run). (B) The measure of coherence is equal to the amplitude of the BOLD signal modulation at the stimulus presentation rate (0.01 Hz for tonotopy, 0.0067 Hz for space mapping) divided by the square root of the power over all other frequencies except the harmonics. Voxels that exceeded a coherence value > 0.3 were then assigned a phase corresponding to the voxel's peak response to the stimuli presented in the cycle. (C) Coherence map used to threshold the phase map. (D) Resulting frequency maps and reversal boundaries (black dotted lines) between the four identified regions. These included: Posterior (CL, CM), Primary (ML, A1, MM), Rostral (Al, R, RM) and Anterior (RTL, RT, RTM). Lh, left hemisphere; Rh, right hemisphere; ant, anterior; lat, lateral.

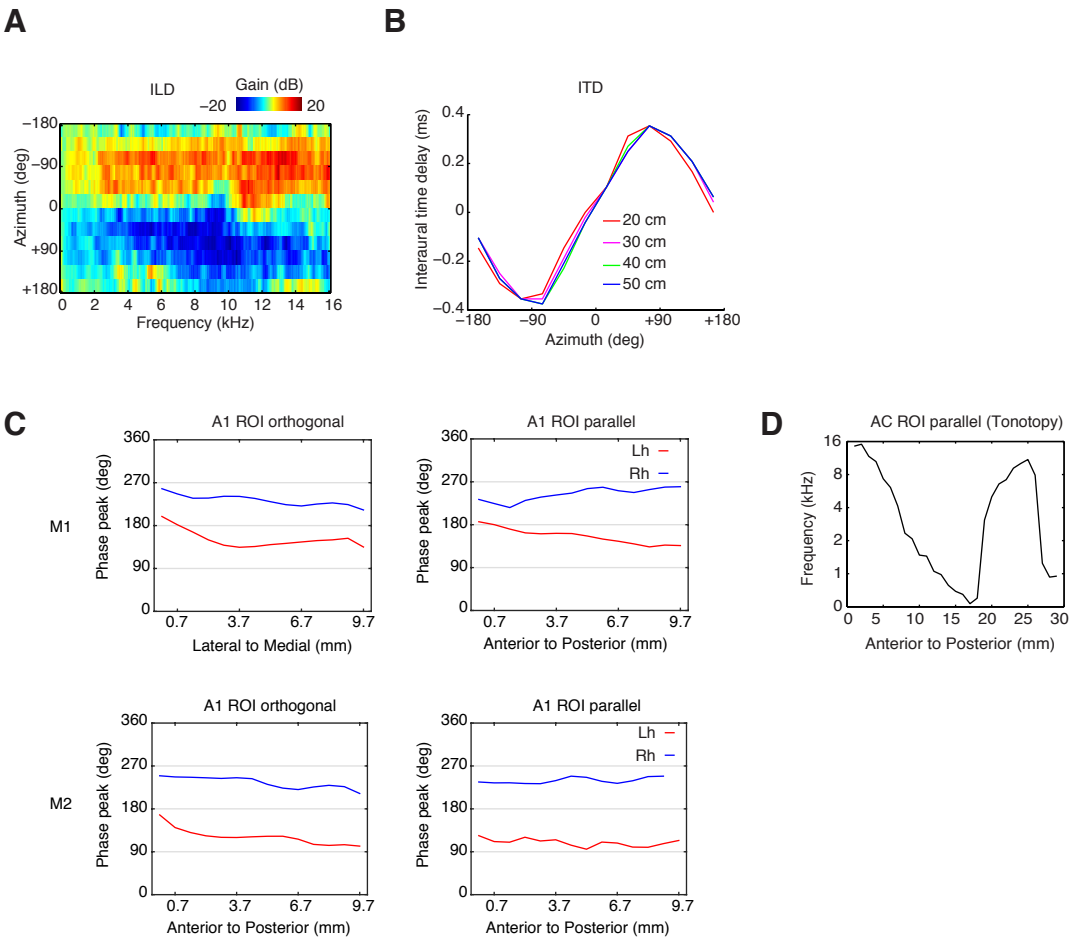

Figure S3. Spatial cues and phase peak response across cortical space
(A) Spectrogram of interaural level differences (L mic − R mic) of spatial stimuli within each sector. (B) Average interaural time delay between left and right stimuli for each sector and distance. (C) Phase peak value along cortical space spanning 10 mm across A1 orthogonal and parallel to the frequency axis shown for M1 (top) and M2 (bottom). (D) Tonotopy phase peak value (normalize to frequency range) along cortical space spanning 30mm across AC parallel to the frequency axis shown for M1 for comparison to flat phase seen in C.

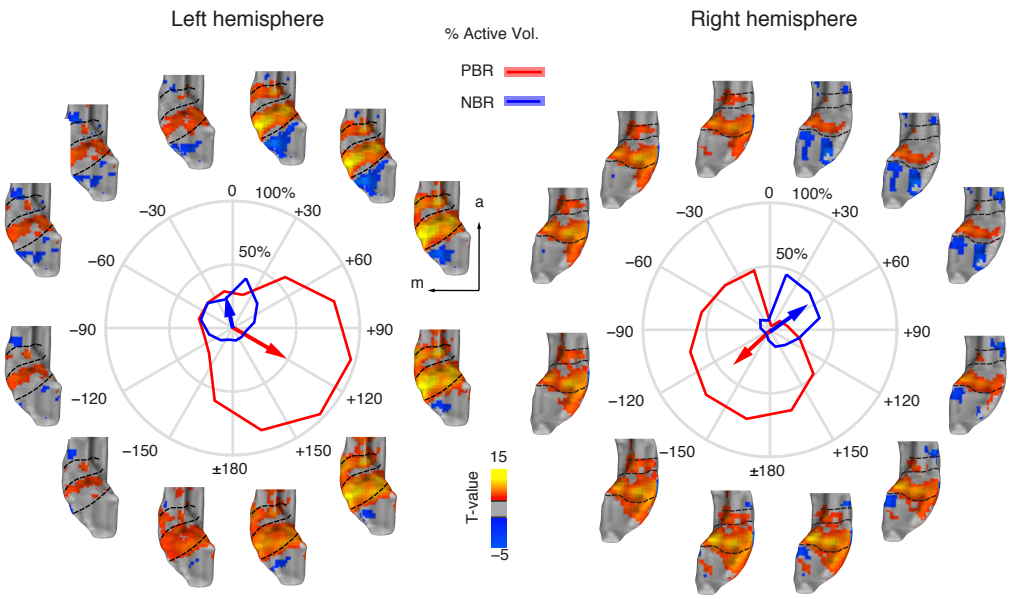

Figure S4. Positive and negative BOLD responses represent opponent hemifields
Activation t-maps with significant positive (red/yellow) and negative (blue) BOLD responses (q FDR < 0.05, p < 10−4, cluster size > 10 voxels). Each map is shown around the corresponding spatial sector in polar plots of each hemisphere of monkey M1. The polar plot shows spatial tuning curves obtained from the spatial spread of the positive (red) and negative (blue) BOLD responses (PBRs and NBRs respectively). Mean resultant vectors points towards the preferred angular direction and the length represents the percentage of active voxels around the mean direction. Negative angles (−180° - 0°) in polar plot represent the left hemifield and positive angles (+180° - 0°) the right hemifield.

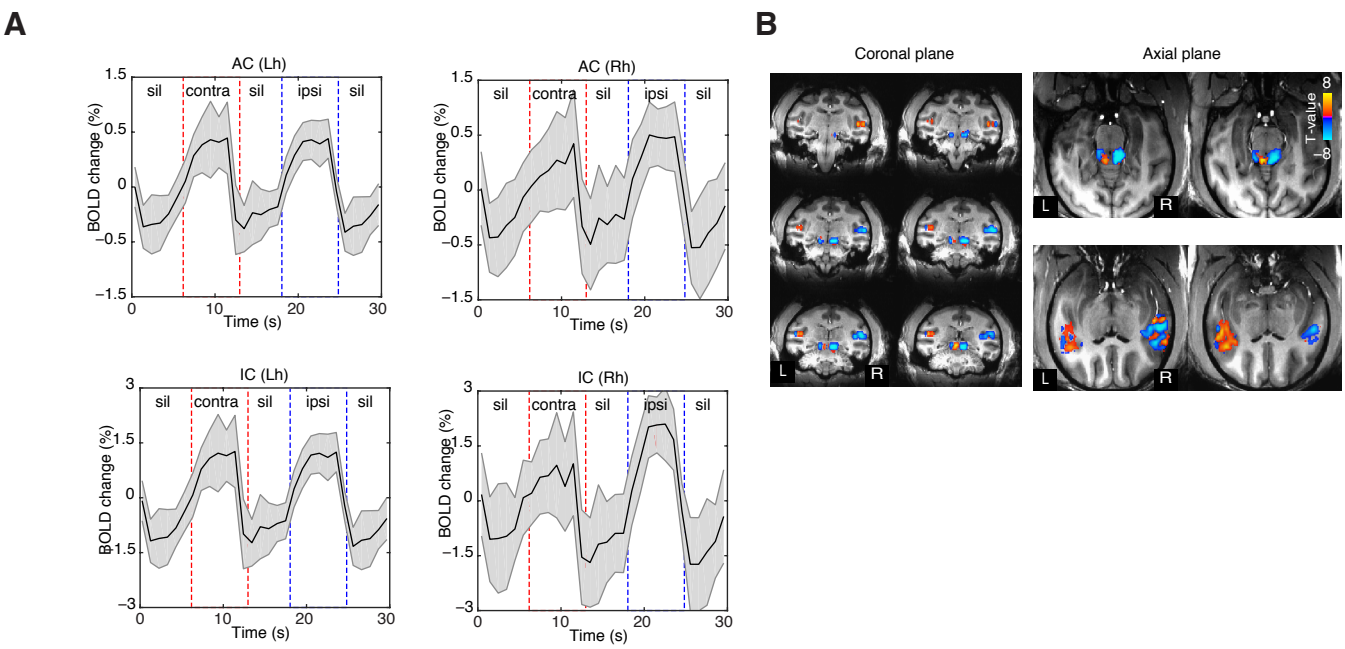

Figure S5. Cortical and subcortical hemifield tuning in awake monkey M4
(A) Average cycles of voxels in auditory cortex (AC) and inferior colliculi (IC) of each hemisphere of monkey M4. Red dashed lines indicate duration periods of sounds presented in the right hemifield and blue dashed duration periods of sounds presented in the left hemifield.(B) Contrast t-maps (q FDR < 0.05, p < 10−2, cluster size > 10 voxels, t-value range ± 8.9) between all left and all right spatial sectors in awake monkey M4. Left image illustrates activations in AC and IC in the saggital plane while right (up) and right (down) illustrates activation in the oblique axial plane of IC and AC respectively. Voxels preferring the left hemifield sectors were mapped as negative (blue-to-cyan) while voxels preferring the right hemifield sectors were mapped as positive (red-to-yellow).

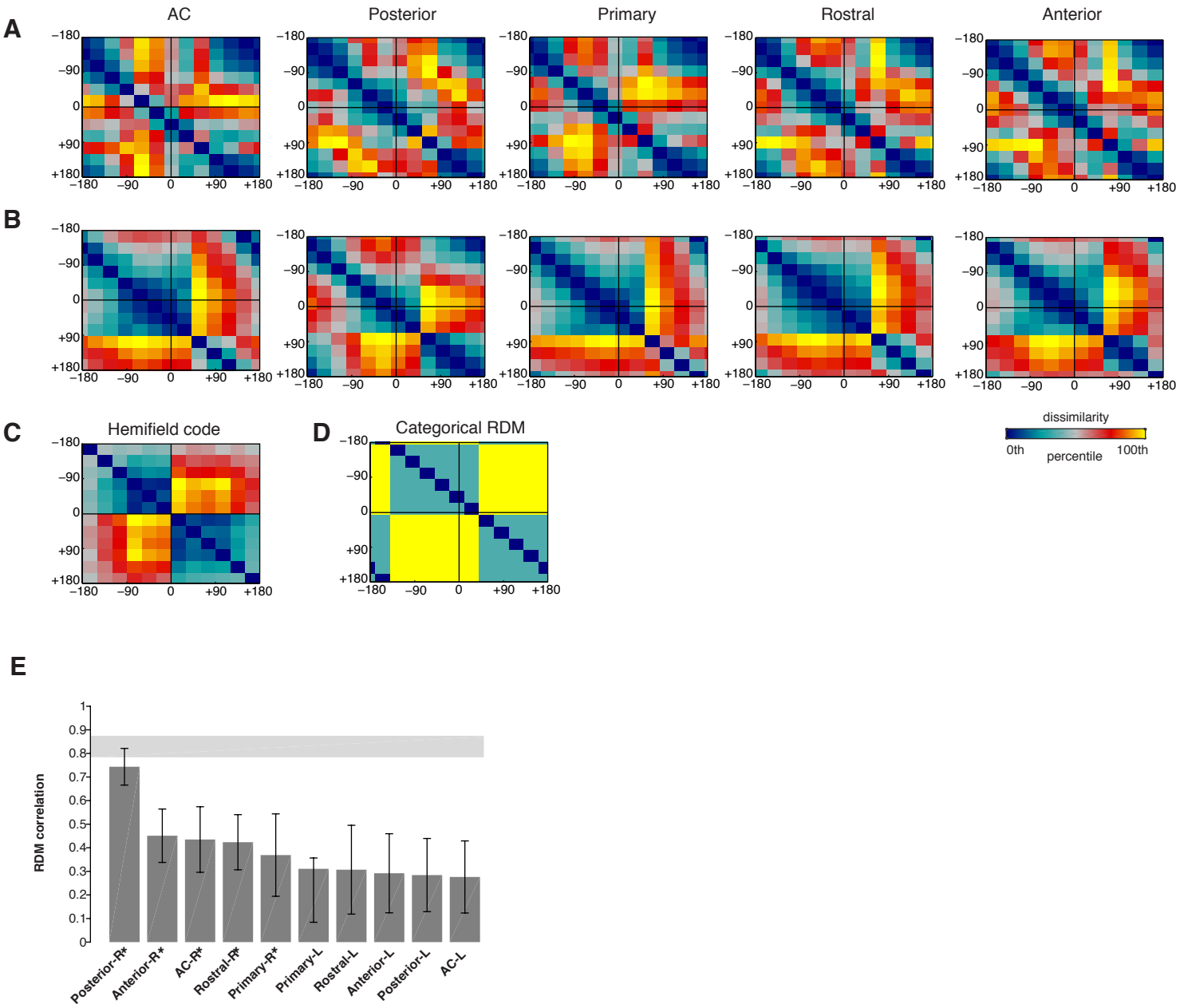

Figure S6. RDM matrices of pairwise dissimilarity values (1 − Pearson R) between BOLD responses to each spatial sector

This analysis was repeated for each cortical field of both left (A) and right (B) hemispheres (including auditory cortex). For the hemifield code RDM (C) we used the ITD delay functions for pair-wise correlations (**Figure S3B**) and linearly combined noisy estimates of the ITD RDMs with a categorical-model RDM (D). (E) Cortical RDMs compared to a hemifield model RDM above. The comparison was conducted using stimulus-label randomization and pair-wise comparisons among cortical RDMs (along with error bars) were based on bootstrap resampling of the stimulus set. Shaded gray bar illustrates the noise ceiling of the model, indicating the expected performance given the noise.

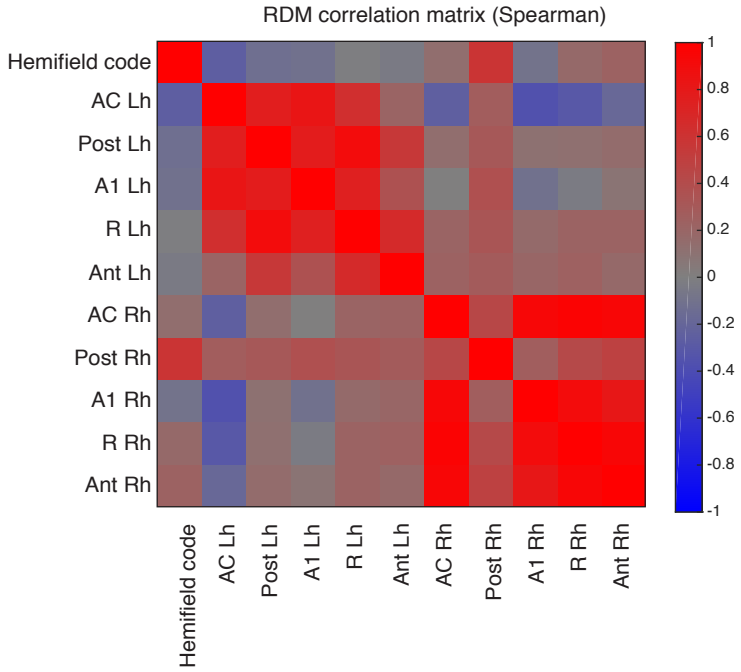

Figure S7. Matrix of RDM correlations (secondary RDM)
We calculated the distance (1 − Spearman correlation coefficient) between RDMs shown in **Figure S5**. Note that the RDM from the right posterior region correlates best with the hemifield code RDM.

A

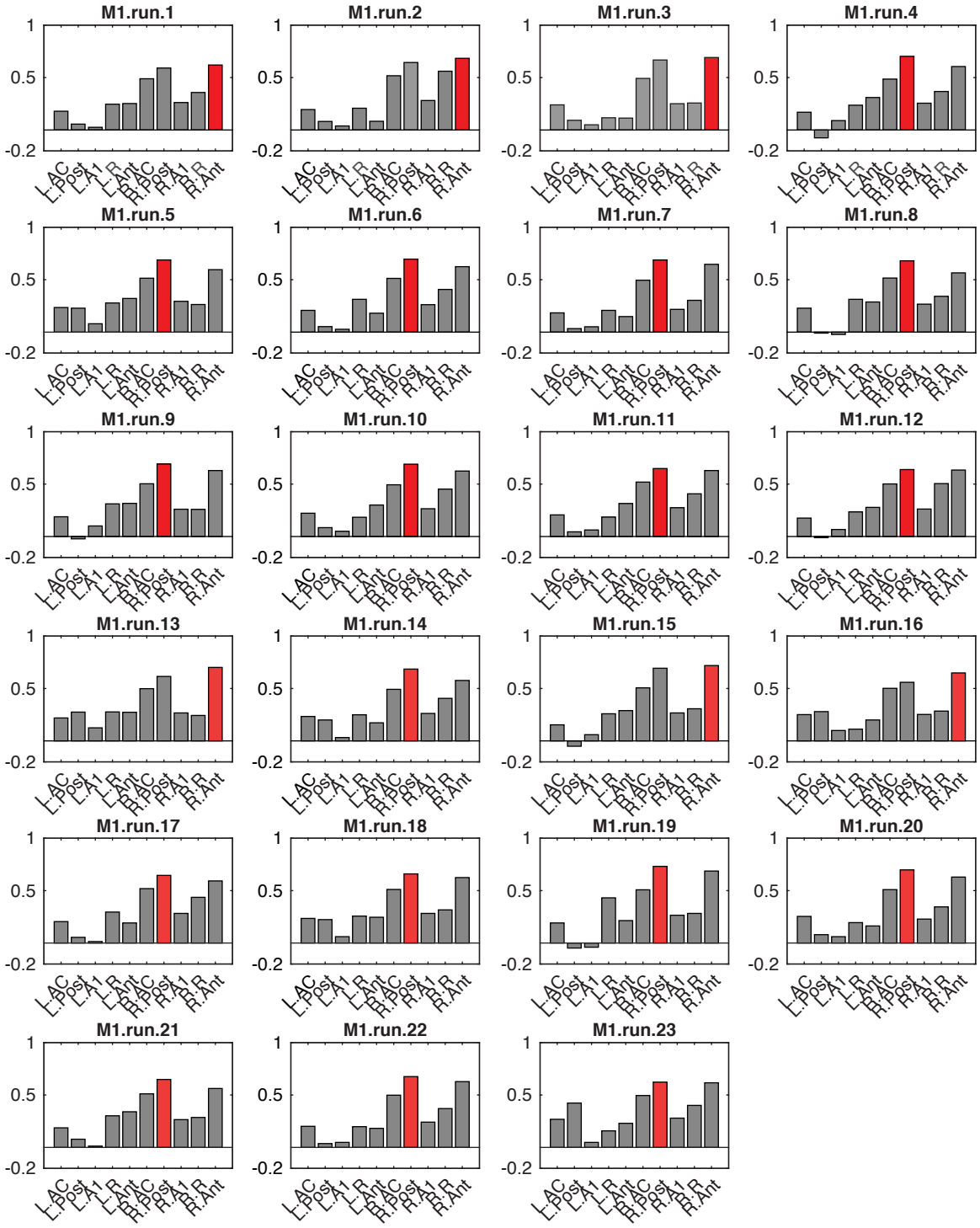
M1.run.1
M1.run.2
M1.run.3
M1.run.4
M1.run.5
M1.run.6
M1.run.7
M1.run.8
M1.run.9
M1.run.10
M1.run.11
M1.run.12
M1.run.13
M1.run.14
M1.run.15
M1.run.16
M1.run.17
M1.run.18
M1.run.19
M1.run.20
M1.run.21
M1.run.22
M1.run.23
1
0.5
-0.2
L.AC
L.Post
L.A1
L.R
L.Ant
R.AC
R.Post
R.A1
R.R
R.Ant

B

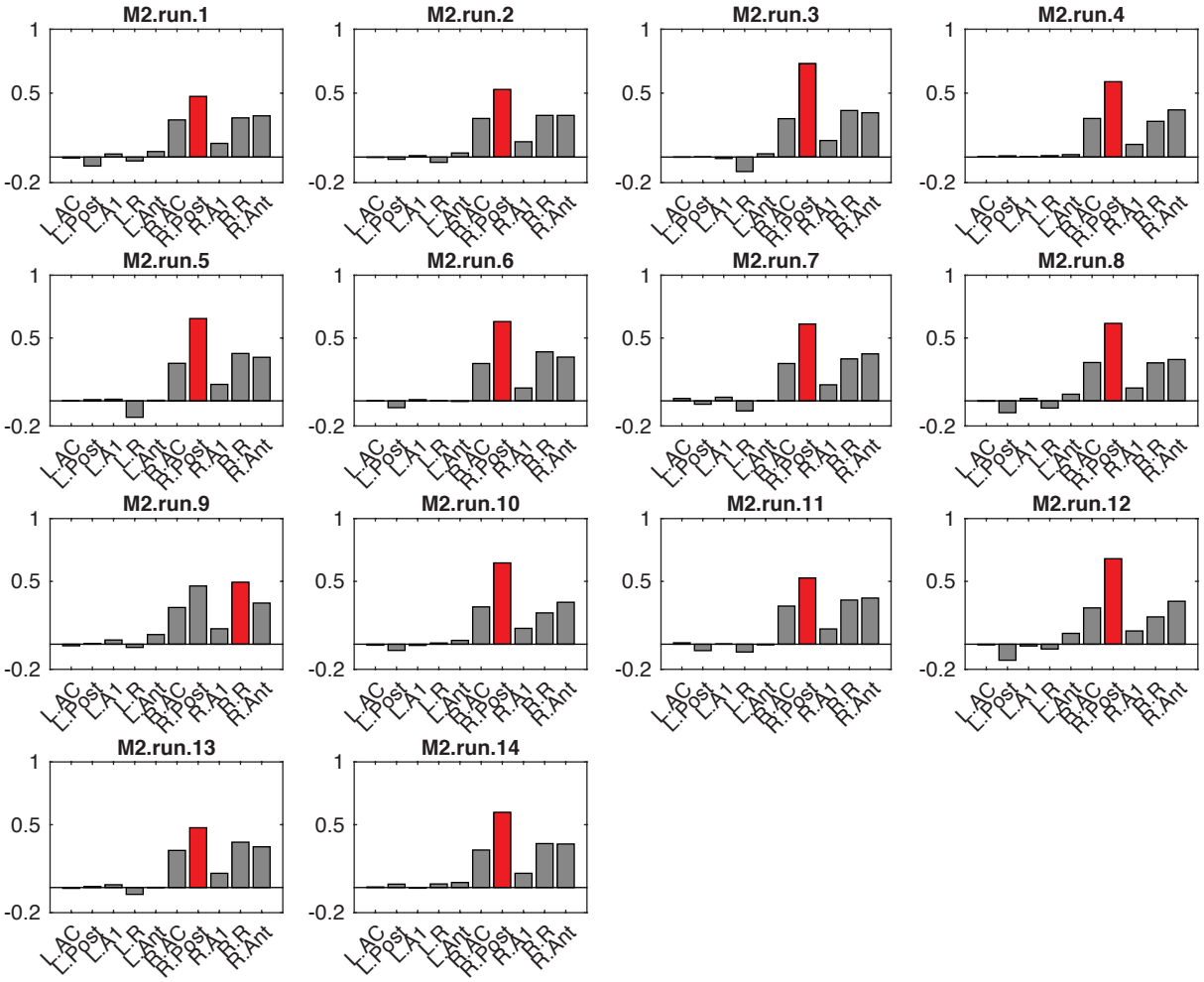
M2.run.1
M2.run.2
M2.run.3
M2.run.4
M2.run.5
M2.run.6
M2.run.7
M2.run.8
M2.run.9
M2.run.10
M2.run.11
M2.run.12
M2.run.13
M2.run.14
1
0.5
-0.2
L.AC
L.Post
L.A1
L.R
L.Ant
R.AC
R.Post
R.A1
R.R
R.Ant

C

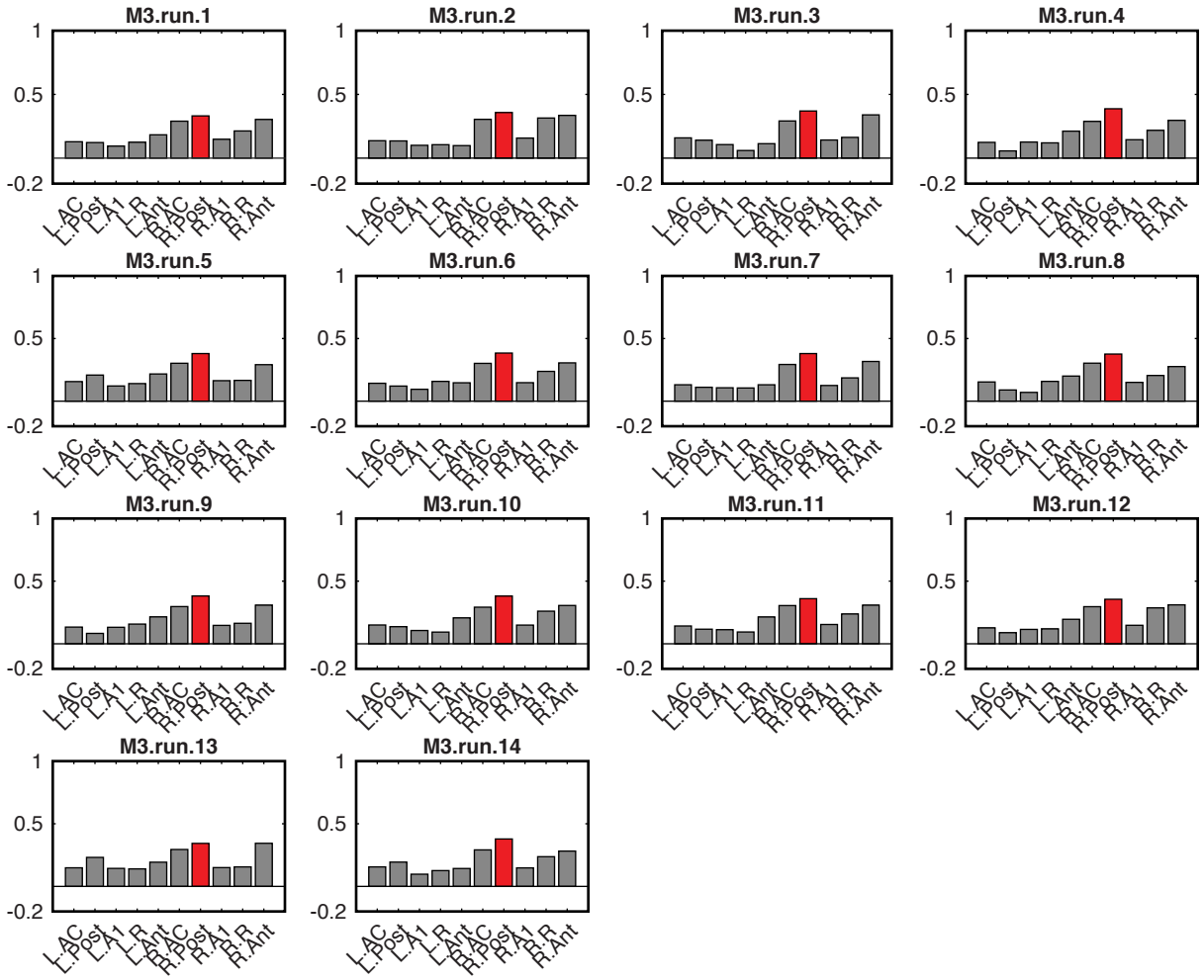
M3.run.1
M3.run.2
M3.run.3
M3.run.4
M3.run.5
M3.run.6
M3.run.7
M3.run.8
M3.run.9
M3.run.10
M3.run.11
M3.run.12
M3.run.13
M3.run.14
1
0.5
-0.2
L.AC
L.Post
L.A1
L.R
L.Ant
R.AC
R.Post
R.A1
R.R
R.Ant

D

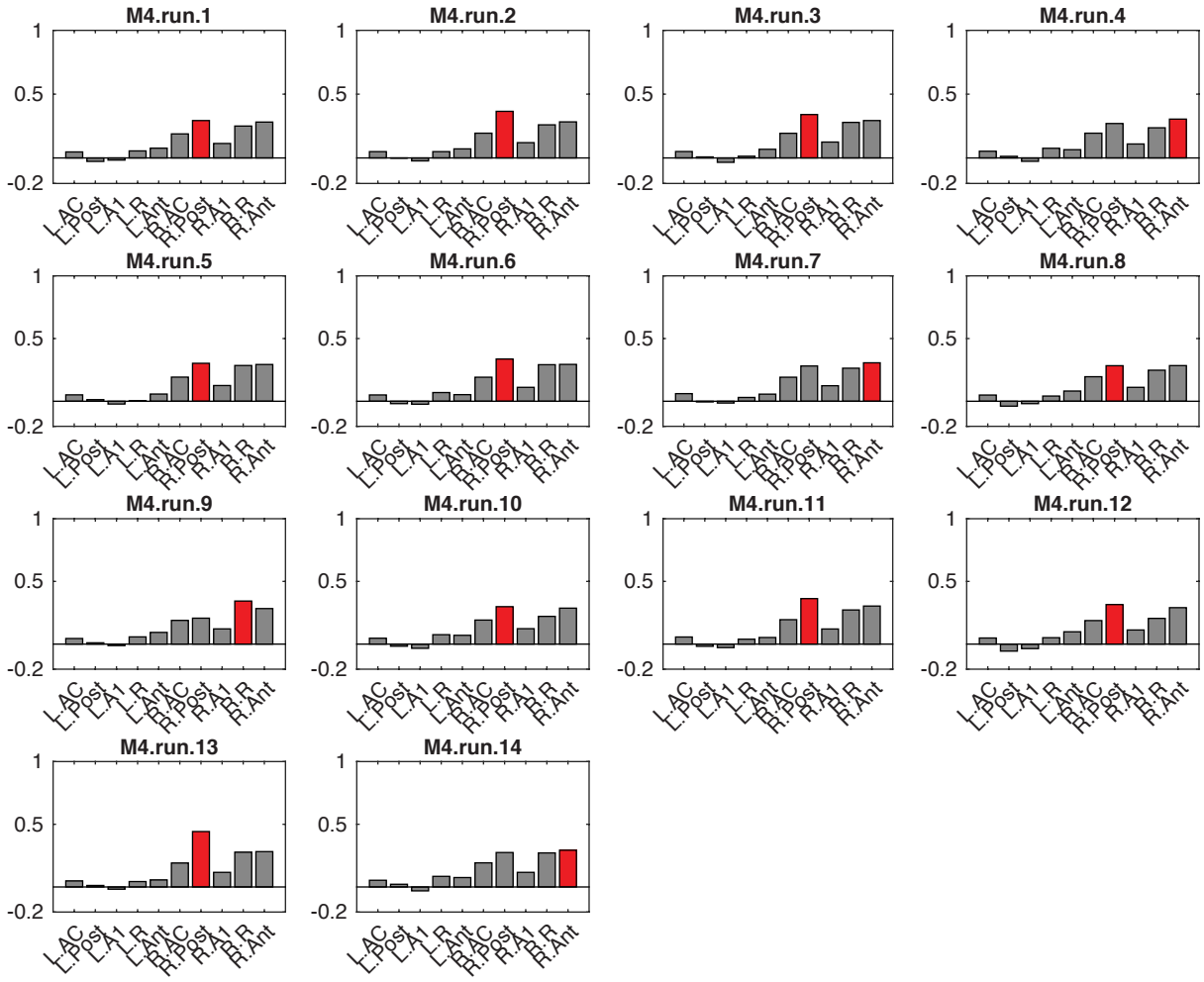
M4.run.1
M4.run.2
M4.run.3
M4.run.4
M4.run.5
M4.run.6
M4.run.7
M4.run.8
M4.run.9
M4.run.10
M4.run.11
M4.run.12
M4.run.13
M4.run.14
1
0.5
-0.2
L.AC
L.Post
L.A1
L.R
L.Ant
R.AC
R.Post
R.A1
R.R
R.Ant

E

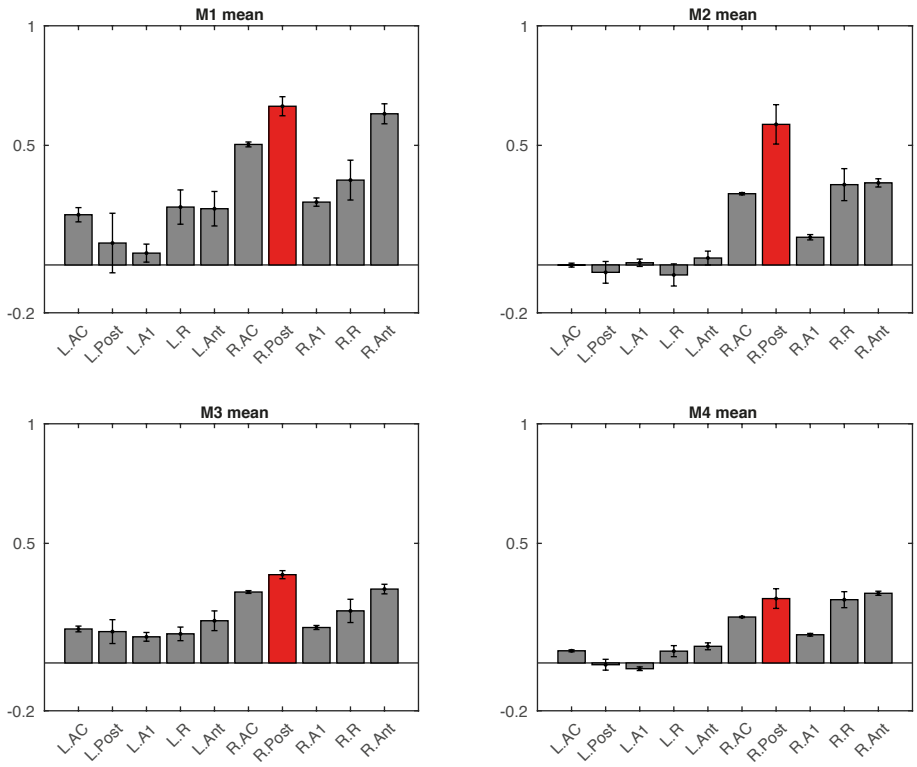

Fig.S8. Spearman's coefficients between each cortical field RDM and hemifield code RDM. (A) Bar histogram of individual Spearman's correlation coeficients between Hemifield code RDM and CF's RDMs from each hemisphere for each individual run of monkey M1. Same plot for M2 (B), M3 (C) and M4 (D). (E) Mean and ± SEM of correlation coefficients for each monkey.